

## A simulation study of RX-mode waves generation in the equatorial plasmasphere

Mohammad Javad Kalae<sup>1\*</sup> and Yuto Katoh<sup>2</sup>

<sup>1</sup>Assistant Professor, Institute of Geophysics, University of Tehran, Tehran, Iran

<sup>2</sup>Associate Professor, Department of Geophysics, Graduate School of Science, Tohoku University, Sendai, Japan

(Received: 7 June 2014, accepted: 7 January 2015)

### Abstract

The generation mechanism of RX-mode waves in the equatorial plasmasphere has not been well understood. The Akebono passing through the storm time geomagnetic equator shows the possibility of the local enhancement of RX-mode waves in association with intense Z-mode waves in the equatorial region. We use the initial parameters inferred from observational data from around the plasma-wave generation region obtained by the Akebono satellite. A comparison of linear growth-rate calculations and simulation results is presented. The results of the simulation show two strong peaks related to the Z-mode and RX-mode waves, while the separation of these wave frequencies is equal to one cyclotron frequency. It is shown that electromagnetic Z- and RX-mode waves could be coupled by a nonlinear interaction.

**Keywords:** RX- mode, simulation, cyclotron frequency, growth rate

### 1 Introduction

Based on simultaneous observations of plasma waves and energetic particles, it has been shown that these emissions are related to unstable particle distributions localized in equatorial regions (Kurth et al., 1980), and some free-energy sources are expected to drive the strong wave-particle interactions in equatorial regions (Green et al., 2004). Energetic electrons with energies in the keV range are frequently observed in the equatorial plasmasphere during geomagnetically active periods. Also, plasma waves are frequently observed in the equatorial plasmasphere. The study of a generation mechanism of Z-mode waves through

instabilities in the equatorial plasmasphere was undertaken by Nishimura et al. (2007) and Kalae (2013) based on a linear theory. Another enhancement is related to the radio emissions that propagate in the LO (Left-Circular Polarization and Ordinary) and RX (Right-Circular Polarization and Extraordinary) mode branches. LO- mode waves can be generated from slow Z-mode waves as a result of a linear mode conversion (Jones, 1977, 1987; Oya 1991; Kalae et al., 2009, 2010). The mode conversion mechanism is likely to explain the kilometric radiations; however, observed intensity of RX- mode waves could not be explained by the

---

\*Corresponding author:

previously proposed mechanism and therefore, the generation mechanism of RX-mode waves in the equatorial region has not been well understood. The purpose of the present study is to investigate the plasma wave enhancements through a numerical simulation aiming at studying the RX-mode wave generation process. For a better understanding of the generation mechanism of plasma waves from instabilities, a comparison of linear growth-rate calculations and simulation results is presented. We use the initial parameters inferred from observational data obtained by the Akebono satellite around the plasma-wave generation region. We discuss and show a possibility of RX-mode wave generation by a wave-particle interaction.

## 2 Instrumentation, Dataset, and Observations

Typical observation events at the generation site of RX-mode waves analyzed in this study were found during the period from 3:20 UT ( $L \approx 2.5$ ) to 4:10 UT ( $L \approx 2.3$ ) on 4 Feb. 1992; see Fig. 1.

The four curves in Figure 1 indicate the characteristic frequencies of the RX-mode cutoff, upper hybrid resonance (UHR), plasma frequency and Z-mode cutoff.

This panel also shows a large inhomogeneity from 03:33 UT to 03:35 UT. The Akebono passing through the storm time geomagnetic equator shows a possibility of the local enhancement of the RX-mode waves in association with intense Z-mode waves in the equatorial region.

## 3 Analysis of linear growth rate

As a first step, we performed the analysis of the linear growth rate. Recently, a statistical study on the global distribution of super thermal electron (0.1-10 keV) fluxes using electron data from THEMIS (Time History of Events and Macroscale Interactions during Substorms) was accomplished by Li et al. (2010). They showed that a significant portion of super thermal electrons can be trapped within the plasmasphere. Inside the plasmasphere, electron fluxes are

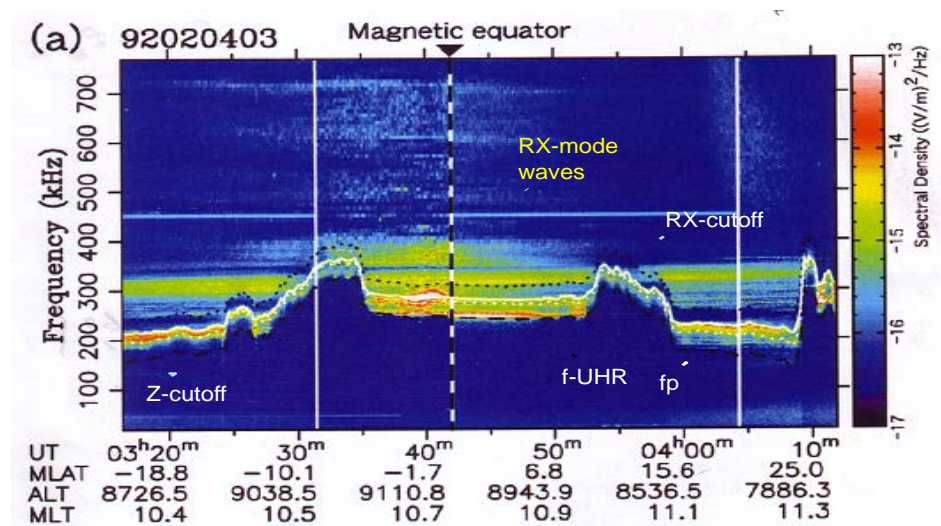


**Figure 1.** Dynamic spectrum of kilometric radiation observed at 3:35-3:50 UT on Feb. 4, 1992, by the Akebono satellite. Four curves indicate the characteristic frequencies of RX-mode cutoff, UHR (f-UHR), plasma frequency (fp) and Z-mode cutoff.

dependent on magnetic activity, energy and  $L$  shell and during strong magnetic activity, the plasmapause moves inward and electrons drift closer to the earth. They also showed that electron fluxes were larger at smaller  $L$  shells for high energy electrons forming an electron ring distribution. We assumed that energetic electrons had a ring distribution (Nishimura et al., 2007; Li et al., 2010; Kalaei et al., 2013) in a momentum space,

$$f(u_{\parallel}, u_{\perp}) = \frac{n_h}{\sqrt{\pi^3 A_{\parallel} A_{\perp}^2 c^3}} \exp\left(-\frac{1}{A_{\perp}^2} \left(\frac{u_{\perp}}{c} - \frac{u_{\perp 0}}{c}\right)^2 - \frac{1}{A_{\parallel}^2} \left(\frac{u_{\parallel}}{c} - \frac{u_{\parallel 0}}{c}\right)^2\right), \quad (1)$$

where  $A^2$  is the variance of the normalized momentum, which corresponds to temperature,  $u_{\parallel 0}$  and  $u_{\perp 0}$  are the average momenta, and  $c$  is the speed of light in free space. The relativistic cyclotron resonance condition is given by

$$\gamma \omega_r - k_{\parallel} u_{\parallel} - n \omega_{ce} = 0, \quad (2)$$

where  $\omega_{ce}$ ,  $\gamma$ , and  $n$  are the cyclotron frequency, the Lorentz factor, and the order of resonance, respectively. The parameters adopted for the ring distribution given by Eq. (1) are  $n_h = 1/cc$ ,  $u_{\perp 0}/c = 0.4 \sim 40$  keV,  $u_{\parallel 0} = 0$ , and  $A = A_{\parallel} = A_{\perp} = 0.1$  (17.5 keV). These

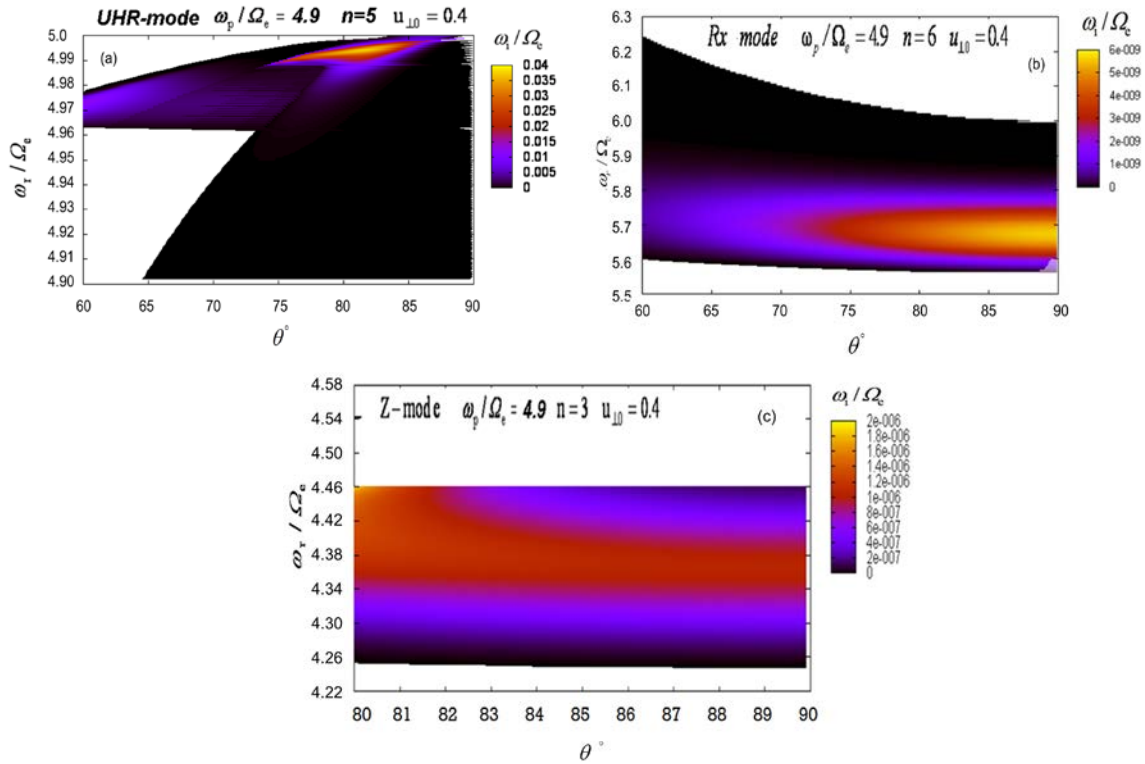


**Figure 2.** The linear growth rate of (a) UHR-mode waves with  $n = 5$ . (b) Rx-mode waves with  $n = 6$ . (c) Z-mode wave with  $n = 3$ ,  $\theta$  is a wave normal angle.

values were estimated from the ring current measurements by Maynard et al. (1996) during disturbed periods. The cold background component,  $n_c = 1000 / cc$ , and  $A = 1.4 \times 10^{-3}$  (1 eV) were estimated in the Akebono/PWS analysis. The adopted ratio of the plasma frequency to the normalized cyclotron frequency has been found to be 4.9. The linear growth rate has been calculated based on the hot-plasma theory (Baldwin et al. 1969):

$$\omega_i = \sum_s \frac{2\pi^2 \omega_{ps}^2}{G \omega^2 n_s} \int du \sum_n \frac{u_{\perp} n \omega_{ce}}{\gamma k_{\perp}} (\alpha_1 J_n^2 + \alpha_2 J_n J_{n+1} + \alpha_3 J_{n+1}^2) (n \omega_{ce} \frac{\partial}{\partial u_{\perp}} + k_{\parallel} u_{\perp} \frac{\partial}{\partial u_{\parallel}}) f_s(u_{\perp}, u_{\parallel}) \cdot \delta(\gamma \omega - k_{\parallel} u_{\parallel} - n \omega_{ce}), \quad (3)$$

where  $n$  is the order of resonance,  $J_n$  is the  $n$ -th Bessel function,  $n_s$  is the electron density of the  $s$  species (cold and hot electrons). The coefficients  $\alpha_1, \alpha_2, \alpha_3$ , and  $G$  are functions of the wave frequency, wavenumber, plasma frequency, cyclotron frequency and the

momentum of the energetic particles, as described by Lee et al. (1979). Fig. 2 shows the growth rate of all wave modes based on linear growth rates in the electron ring distribution. Panel (a) shows the growth rate of UHR-mode waves in the wave-number–frequency space for  $n=5$ . The growth rate is approximately  $4.0 \times 10^{-2} \omega_{ce}$  for  $\theta=90^\circ$ . However, frequencies in resonance are strongly limited. Panel (b) shows the growth rate of RX mode waves for  $n=6$  and panel (c) shows the wave growth rate of Z-mode for  $n=3$ , the maximum growth rate is approximately  $2.0 \times 10^{-6} \omega_{ce}$  with  $\omega_r / \omega_{ce} \approx 4.46$  and  $\theta=90^\circ$ . The group velocity of this wave, which is also nearly perpendicular to the magnetic field, is approximately  $0.48c$ . These waves can resonate with keV-energy electrons around  $\omega \approx n \omega_{ce}$ . For  $\omega_p / \omega_{ce} = 4.9$ , third-order resonances show the highest growth rate. For  $n \leq 2$  the resonance condition is not satisfied for Z-mode waves and for  $n \geq 4$ , it requires relativistic electrons with energies in excess of 100 keV. The

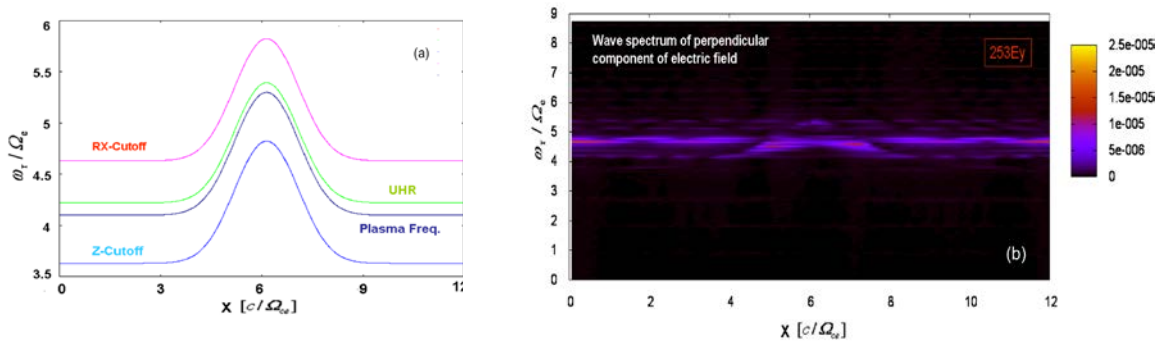


**Figure 3.** (a) The profiles of plasma frequency, UHR, Z-cutoff and RX-cutoff used in the simulation model. (b) The wave spectrum of perpendicular component of electric field showing that the UHR, Z-mode and RX-mode waves are excited.

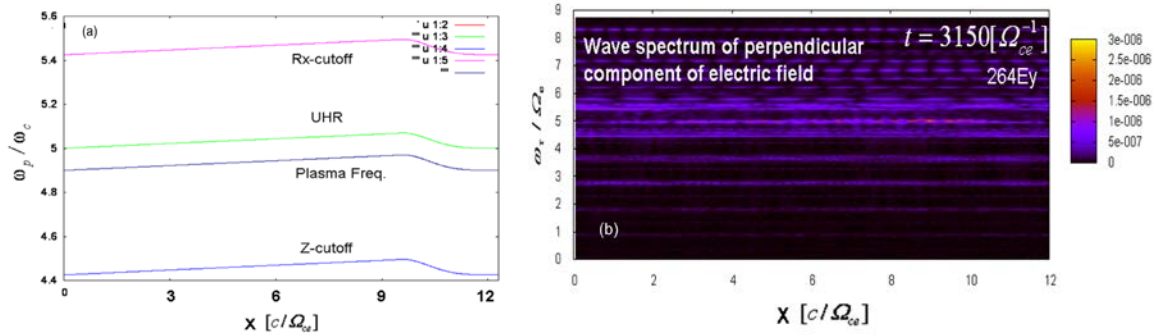


**Figure 4.** (a) The profiles of plasma frequency, UHR, Z-cutoff and RX-cutoff used in the simulation model. (b) The wave spectrum of the perpendicular component of the electric field showing that the UHR, Z-mode and RX-mode waves are excited.

energy contained in the particle population is much less than 1–10 keV and the growth rate is more than one order of magnitude smaller. A possibility of the enhancements of the Z-mode waves is the existence of energetic electrons with energies of some tens of keV that are confined around the geomagnetic equator. The results of the growth rate calculation show that various wave modes are simultaneously excited in the presence of the ring-type velocity distribution.

However, the maximum linear growth rate of RX-mode waves is weak and the hypothesis of the generation mechanism of RX-mode waves from instabilities makes it difficult to explain the generation of the observed strong RX-mode radio emissions. In the next section, we further study the wave generation process by conducting numerical experiments by assuming the same initial conditions used in the computation.

#### 4 Simulation Model

The electron hybrid model is able to describe the energy transfer between

high-energy electrons and plasma waves propagating in a medium of cold electrons and enables us to examine interactions between relativistic electrons and plasma waves. A description of the model and the basic equations used in this model are presented by Katoh et al. (2005).

We carried out a one-dimensional simulation. The wave characteristics resulting from the competition of wave excitation processes of waves of different modes is discussed here. Each physical value is normalized to render it a dimensionless quantity; i.e., time is normalized by cyclotron frequency  $\omega_{ce}$ , and velocity and length are normalized by the speed of light  $c$  and  $c/\omega_{ce}$ , respectively. The physical system is aligned along the  $X$  axis and the external magnetic field is assumed to be oriented perpendicular to the  $X$  axis. Table 1 gives the initial parameters used in the present study. We used a ring distribution, with  $n_h/n_c = 10^{-3}$ , where  $n_h$  and  $n_c$  are the number densities of the hot and cold background plasmas, respectively.

**Table 1.** The initial parameters used in the present study.

Grid spacing $\Delta x$	$6 \times 10^{-3} c / \omega_{ce}$
Time step $\Delta t$	$4.5 \times 10^{-3} \omega_{ce}^{-1}$
Number of grids in X-axis	2048
Number of time steps	700,000
Total simulation time	$3150 \omega_{ce}^{-1}$

## 5 Simulation results and discussions

As the first step, we considered a spatial variation of the plasma frequency from 4.1 to  $5.3 \omega_{ce}$  in the simulation system as shown in Fig. 3a. The range of the variation of the local plasma frequency is determined by referring to the observation results (Fig.1). The four curves in Fig. 3a indicate the characteristic frequencies of RX-mode cutoff, UHR, plasma frequency and Z-mode cutoff in the simulation system. Fig. 3b shows a wave spectrum of  $E_y$  component of the electric field obtained from simulation results, showing the enhancement of Z-mode and RX-mode waves. Enhancement of a strong Z-mode wave has been seen in plasma frequencies within  $4.5 \sim 5 \omega_{ce}$ .

For the next step, we focused on the wave enhanced region and the plasma frequency was chosen from 4.9 to  $4.97 \omega_{ce}$  as shown in Fig. 4a; the four curves indicate the characteristic frequencies of RX-mode cutoff, UHR, plasma frequency and Z-mode cutoff in the simulation system. Fig. 4b shows a wave spectrum of  $E_y$  component at  $t = 3150 \omega_{ce}^{-1}$  that indicates the simultaneous enhancement of Z-mode

and RX-mode waves.

Fig. 5 shows the wave frequency spectrum of  $E_y$  component of electric field at the location of  $X = 0.3 c \omega_{ce}^{-1}$  where the local plasma frequency is  $4.9 \omega_{ce}$ . Two strong peaks are related to Z-mode and RX-mode waves, while the separation of these wave frequencies is exactly equal to one cyclotron frequency. In Fig. 6, the position of each wave mode in the  $\omega$ -k diagram is shown where the plasma frequency is  $4.9 \omega_{ce}$ ; we can see that the wave frequency difference is equal to one cyclotron frequency. By referring to the linear growth rate of RX-mode wave, the wave frequency of the positive growth rate of RX-mode is found above  $5.55 \omega_{ce}$  as shown in Fig. 2b, whereas the frequency range of the enhanced RX-mode waves from simulation result appears to be about  $5.46 \omega_{ce}$ . There is a possibility that the RX-mode wave is excited by a nonlinear interaction. A nonlinear coupling condition has been proposed by Oya (1971), given by

$$(\omega_2 - \omega_1) - (k_{2\parallel} - k_{1\parallel}) \cdot V_{\parallel} = n \omega_{ce}, \quad (4)$$

where  $\omega_2$  and  $\omega_1$  are wave frequencies and  $k_{2\parallel}$ ,  $k_{1\parallel}$  are parallel components of the wave vectors of the two modes;  $V_{\parallel}$  being the parallel velocity component of the particles. For the case of  $\theta=90^\circ$ , the parallel component of the wave vector becomes zero and the condition is described by

$$(\omega_2 - \omega_1) = n \omega_{ce}. \quad (5)$$

Table 2 shows the summary of characteristic frequencies and simulation

results, where  $\Delta\omega$  and  $\Delta k$  are resolution of the wave frequency and wave vector determined from the Nyquist frequency derived from the Fast Fourier transform (FFT) analysis and the resultant wave number resolution. The ratios of the two electric field components of each wave obtained from both dispersion relation and simulation results are also shown. We analyzed the frequency separation of Z-mode and RX-mode branches as a function of wave number as shown in Fig. 7. Table 2 shows that the wave numbers of Z- and RX-modes are the same. Fig. 7 reveals that the frequency separation at the observed wave number range is equal to one cyclotron frequency. The evidence emphasizes the possibility that the RX-mode wave is generated by nonlinear interactions between particles and Z-mode waves.

## Conclusions

In simultaneous observations of localized plasma waves and energetic particles in

the equatorial regions, energetic electrons are frequently observed within the keV energy range in the equatorial plasmasphere during geomagnetically active periods. As shown in Fig.1, the Akebono passing through the storm time geomagnetic equator shows the possibility of the local enhancement of RX-mode waves in association with intense Z-mode waves in the equatorial region. In the first section, the linear growth rate of the RX-mode waves has been calculated under the cyclotron interaction process. The results of the linear growth rate showed the simultaneous enhancement of Z-, UHR- and RX- mode waves through the instability driven by the ring-type velocity distribution. In the second section, the generation of RX-mode wave was considered by performing the simulation. Simulation results showed an enhancement of RX-mode wave as well as an enhancement of Z-mode. The results showed that the frequency

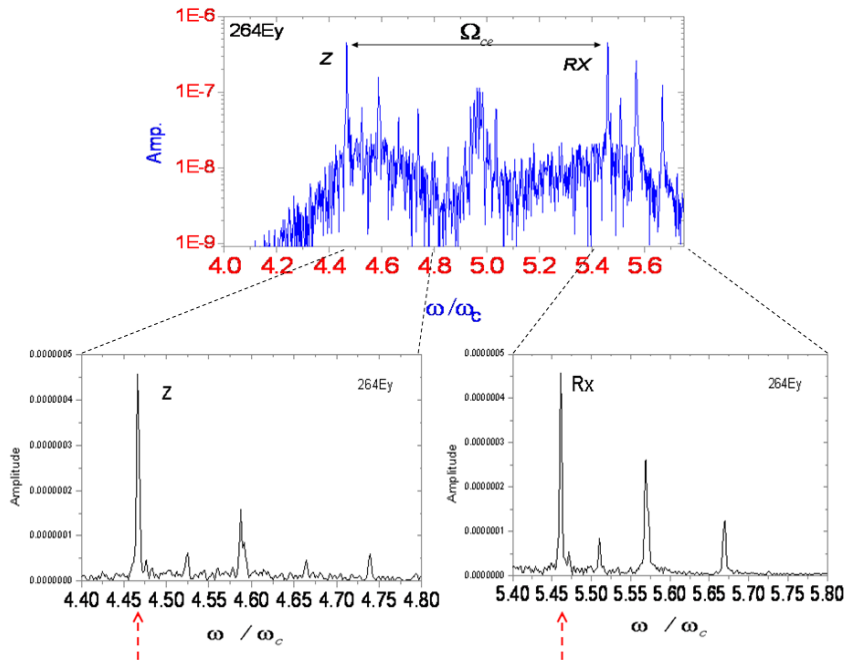


**Figure 5.** The spectrum of wave frequency of Ey electric field distribution.

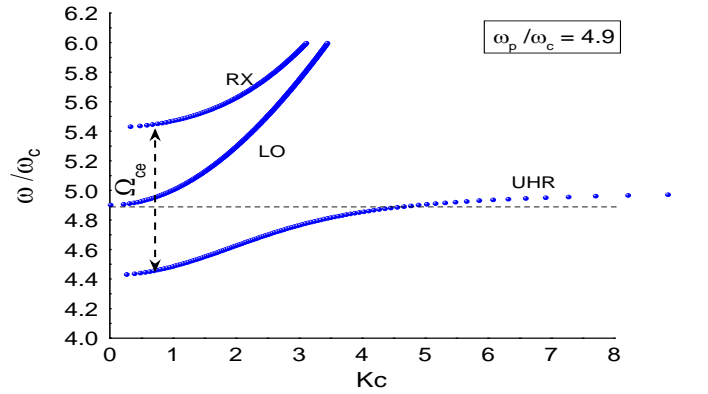


**Figure 6.** The  $\omega$ - $k$  diagram with  $\theta=90^\circ$ . The position of Z-mode and RX-mode waves are indicated by circle marks that show the wave frequency difference is one cyclotron frequency.

separation of wave frequencies of Z-mode and RX-mode waves was exactly equal to one cyclotron frequency. Therefore, by referring the results of the linear growth rate, the simulation results and the nonlinear coupling condition, we suggest a possibility that energetic electrons with energies of some tens of keV confined around the geomagnetic equator are responsible for the observed enhancements of Z- and RX-mode waves and that wave particle interaction

generates RX-mode waves through nonlinear wave particle interactions. In the present study, we assumed a uniform magnetic field in the simulation system. A mirror motion of energetic electrons can be treated by assuming the field-aligned inhomogeneity of the background magnetic field intensity. Such works of wave generation processes of a variety of wave modes in the magnetosphere are important for our future study.

**Table 2.** Some characteristics of initial plasma waves and results of simulation, including: Plasma frequency

( $X_p = \frac{\omega_p}{\omega_{ce}}$ ), Z-cutoff ( $X_{Z-cutoff} = \frac{\omega_{Z-cutoff}}{\omega_{ce}}$ ) and RX-cutoff frequencies, also frequencies of UHR-mode, Z-mode and RX-mode exciting waves with their K vectors; with ratio of two components of each mode obtained from simulation results and dispersion relation. All frequencies are normalized by cyclotron frequency.

$X_p$	$X_{Z-cutoff}$	$X_{RX-cutoff}$	$X_{UHR}$	$X_Z \pm \Delta X_Z$	$K_Z \pm \Delta K_Z$	$X_{RX} \pm \Delta X_{RX}$	$K_{RX} \pm \Delta K_{RX}$	(Dispersion relation)		(Simulation)	
								$(E_x / E_y)_Z$	$(E_x / E_y)_{RX}$	$(E_x / E_y)_Z$	$(E_x / E_y)_{RX}$
4.9	4.425	5.425	5.001	$4.465 \pm 0.005$	$0.81 \pm 0.06$	$5.465 \pm 0.005$	$0.87 \pm 0.06$	1.056	0.92	1.1	0.96

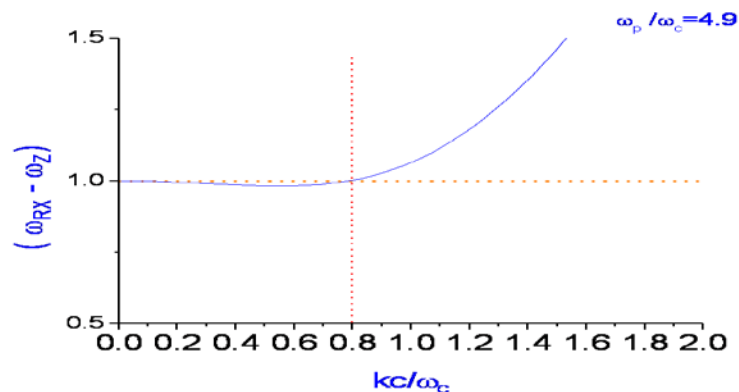


**Figure 7.** The separation of wave frequencies of Z-mode and RX-mode waves' branches vs. wave number  $k$ , based on  $\omega$ - $k$  diagram.

### Acknowledgments

The computation was performed with computer facilities at Research Institute for Sustainable Humansphere and Academic Center for Computing and Media Studies of Kyoto University, the Solar-Terrestrial Environment Laboratory of Nagoya University, and Cyberscience Center of Tohoku University.

The authors would like to acknowledge the financial support of University of Tehran for research under the grant number 28905/1/03.

### References

- Baldwin, D. E., Bernstein, I. B. and Weenink, M. P. H., 1969, Kinetic theory of plasma waves in a magnetic field: *Advances in plasma physics*, edited by Simon, A. and Thompson, W.B., **3**, pp. 1-125.
- Buneman, O., 1959, Dissipation of currents in ionized media: *Phys. Rev.*, **115**, 503-51.
- Eliasson, B., and Shukla, P. K., 2003, Simulation study of radiation generation by upper-hybrid waves in space plasmas: *J. Phys. Lett.*, **A312**, 91-96.
- Green, J. L., Boardsen, S., Fung, S. F., Matsumoto, H., Hashimoto, K., Anderson, R. R., Sandel, B. R. and Reinisch, B. W., 2004, Association of kilometric continuum radiation with plasmaspheric structures: *J. Geophys. Res.*, **109**, A03203, doi: 10.1029/2003JA 010093.
- Jones, D., 1977, Mode-coupling of Z-mode waves as a source of terrestrial kilometric and Jovian decametric radiations: *Astron. Astrophys.*, **55**, 245-252.
- Jones, D., Calvert, W., Gurnett, D. A. and Huff, R. L., 1987, Observed beaming of terrestrial myriametric radiation: *Nature*, **328**, 391-395.
- Kalaei, M. J., Ono, T., Katoh, Y., Iizima, M. and Nishimura, Y., 2009, Simulation of mode conversion from UHR-mode wave to LO-mode wave in an inhomogeneous plasma with different wave normal angles: *Earth Planets and Space*, **61**, 1243-1254.
- Kalaei, M. J., Katoh, Y., Kumamoto, A., Ono, T., and Nishimura Y., 2010, Simulation of mode conversion from upper-hybrid waves to LO-mode waves in the vicinity of the Plasmopause: *Annales Geophysicae*, **28**, 1289-1297.
- Kalaei, M. J., Katoh, Y., and Ono, T., 2013, A simulation study of the

- plasma wave enhancements in the earth's equatorial plasmasphere: *Earth, Moon and Planets*, **110**, 131-141.
- Katoh, Y., Ono, T., and Iizima, M., 2005, Numerical simulation of resonant scattering of energetic electrons in the outer radiation belt: *Earth, Planets and Space*, **57**, 117-124.
- Kurth, W. S., Frank, L. A., Ashour-Abdalla, Gurnett, M., D. A., and Burek, B. G., 1980, Observation of a free-energy source for intense electrostatic waves: *Geophys. Res. Lett.*, **7**, 293-296.
- Lee, L. C., Wu, C. S., Freud, H. P., Dillenburg, D., and Goedert, J., 1979, Excitation of high-frequency waves with mixed polarization by streaming energetic electrons: *J. Plasma Phys.*, **22**, 277-288.
- Li, W., Thorne, R. M., Bortnik, J., Nishimura, Y., Angelopoulos, V., Chen, L., McFadden, J. P., and Bonnell, J. W., 2010, Global distributions of superthermal electrons observed on the THEMIS and potential mechanisms for access into the plasmasphere: *J. Geophys. Res.*, **115**, 1-14.
- Maggs, J., and Geomagn, J., 1978, Theory of electromagnetic waves on auroral fieldlines: *J. Geomag. Geoelec.*, **30**, 273-387.
- Maynard, N. C., Burke, W. J., Basinska, E. M., Erickson, G. M., Hughes, W. J., Singer, H. J., Yahnin, A. G. Hardy, D. A., Mozer, F. S., 1996, Dynamics of the inner magnetosphere near times of substorm onsets: *J. Geophys. Res.*, **101**, 7705-7736.
- Nishimura, Y., Ono, T., Iizima, M., Shinbori, A., and Kumamoto, A., 2007, Generation mechanism of Z-mode waves in the equatorial plasmasphere: *Earth, Planets Space*, **59**, 1027-1034.
- Oya, H., 1991, Studies on plasma and plasma waves in the plasmasphere and auroral particle acceleration region, by PWS on board the EXOS-D (Akebono) Satellite: *J. Geomag. Geoelectr.*, **43**, 369-393.